

Mechanisms of delayed ischemia/reperfusion evoked ROS generation in the hippocampal CA1 zone of adult mouse brain slices

Yuliya V. Medvedeva

University of California Irvine

Edward Sharman

University of California Irvine

John H. Weiss

jweiss@uci.edu

University of California Irvine

Article

Keywords: hippocampal slice, mitochondria, mitochondrial hyperpolarization, Zn^{2+} , MCU, oxygen glucose deprivation

Posted Date: April 22nd, 2025

DOI: <https://doi.org/10.21203/rs.3.rs-5640324/v1>

License:  This work is licensed under a Creative Commons Attribution 4.0 International License.

[Read Full License](#)

Additional Declarations: No competing interests reported.

Abstract

ROS overproduction is an important contributor to delayed ischemia/reperfusion induced neuronal injury, but relevant mechanisms remain poorly understood. We used oxygen-glucose deprivation (OGD)/reperfusion in mouse hippocampal slices to investigate ROS production in the CA1 pyramidal cell layer during and after transient ischemia. OGD evoked a 2-stage increase in ROS production: 1st – an abrupt increase in ROS generation starting during OGD followed by a marked slowing; and 2nd – a sharp ROS burst starting ~ 40 min after reperfusion. We further found that a slight mitochondrial hyperpolarization occurs shortly after OGD termination. Consequently, we showed that administration of low dose FCCP or of FTY720 (both of which cause mild, ~ 10%, mitochondrial depolarization), markedly diminished the delayed ROS burst, suggesting that mitochondrial hyperpolarization contributes to ROS production after reperfusion. Zn^{2+} chelation after OGD withdrawal also substantially decreased the late surge of ROS generation – in line with our prior studies indicating a critical contribution of Zn^{2+} entry into mitochondria via the mitochondrial Ca^{2+} uniporter (MCU) to mitochondrial damage after OGD. Thus, reperfusion-induced mitochondria hyperpolarization and mitochondrial Zn^{2+} accumulation both contribute to mitochondrial ROS overproduction after ischemia. As these events occur after reperfusion, they may be amenable to therapeutic interventions.

Introduction

Brain ischemia is a leading cause of disability and mortality in the aging population. After brief ischemic episodes, many vulnerable neurons like hippocampal pyramidal neurons often initially recover but die hours to days later [1, 2]. Considerable evidence supports the view that oxidative stress due to ROS overproduction is a key contributor to the delayed neuronal injury, damaging tissue and contributing to activation of cell death pathways [3, 4]. Consequently, it was suggested that substantial amounts of ROS are produced after restoration of blood flow (reperfusion), and thus oxygen and glucose supply. Unfortunately, antioxidants have shown little benefits in clinical trials, likely due to inadequate access to the sites of damage. Therefore, elucidating the mechanisms underlying ROS overproduction is essential for identifying new therapeutic targets.

Information currently available about the dynamics and mechanisms of post-ischemic ROS generation is insufficient for the development of therapeutic approaches. While several possible contributors have been proposed including mitochondria, NADPH oxidase (NOX) and xanthine oxidase [5–7], mitochondria are believed to be the dominant source responsible for 80–90% of post-ischemic ROS production [8, 9].

Neuronal Ca^{2+} overload has long been considered a major player in ischemic ROS production [5, 10, 11] however the mechanism was not clearly understood. A number of studies investigating Ca^{2+} effect on mitochondria laid the base for a recently proposed hypothesis highlighting Ca^{2+} -mediated mitochondrial hyperpolarization as a key contributor to reperfusion-associated ROS overproduction [9]. Specifically, Ca^{2+} accumulates in neurons during ischemia and quickly enters mitochondria through the

mitochondrial Ca^{2+} uniporter (MCU) [12–14]. Under physiological conditions of increased energy demand, elevated mitochondrial Ca^{2+} accumulation increases activity of multiple mitochondrial proteins involved in oxidative phosphorylation consequently leading to transient moderate increases in mitochondrial respiration and ROS production [9, 15–17]. However, ischemic conditions, that lead to strong cytoplasmic and, thus, mitochondrial Ca^{2+} overload likely result in considerable overactivation of the respiratory proteins, and probably lead to a hyperactive state of the electron transport chain (ETC) upon reintroduction of oxygen [9]. This, in turn, likely results in prolonged mitochondrial hyperpolarization and a burst of ROS generation, as several studies have found that mitochondrial hyperpolarization (when the mitochondrial membrane potential, $\Delta\Psi_m$, is more negative than ~ -140 mV) causes an exponential increase in ROS production [18, 19].

Another factor likely contributing to ischemic ROS overproduction is mitochondrial Zn^{2+} accumulation. Zn^{2+} accumulates in selectively vulnerable neurons after ischemia [20, 21], and enters mitochondria via the MCU where it stays for prolonged periods and contributes to mitochondrial dysfunction [22–26]. Multiple studies using cell culture have shown that Zn^{2+} accumulation in mitochondria is a highly potent trigger of ROS generation [27–31].

Our recent studies using an ischemia model in brain slices have shown that both Ca^{2+} and Zn^{2+} accumulate in mitochondria of hippocampal CA1 neurons during ischemia; next, when mitochondria depolarize due to insufficient supply of ATP, these ions are released back to the cytoplasm; finally, upon reperfusion and recovery of $\Delta\Psi_m$, both Ca^{2+} and Zn^{2+} re-enter mitochondria. Ca^{2+} seem to be cleared from mitochondria relatively quickly, but Zn^{2+} stays there for a prolonged period (more than 1 hour) [24–26]. We suggest that the persistent mitochondrial Zn^{2+} accumulation, which occurs in CA1 neurons after ischemia/reperfusion, is an important contributor to ROS overproduction.

Our study uses an *ex vivo* oxygen/glucose deprivation (OGD) model of ischemia/reperfusion in acute brain slices loaded with a ROS sensitive indicator to assess the dynamics of ROS generation during and after short ischemia in the CA1 hippocampal region. We observed a sharp increase in ROS generation during and for several minutes after the ischemic episode. However, after this burst, ROS production considerably subsides for 20–30 min, before the occurrence of a second delayed sharp surge in ROS generation. Next, we utilized pharmacological interventions delivered after the ischemic episode to examine mechanisms contributing to the surge in ROS generation after reperfusion. We found that delayed mitochondrial hyperpolarization, and Zn^{2+} uptake to mitochondria through the MCU are both major contributors to post-ischemic ROS overproduction. Interventions targeting these mechanisms can be delivered after restoration of blood flow and, thus, might represent promising therapeutic approaches to decrease delayed brain injury after ischemia.

Materials and Methods

Animals.

All studies were performed according to the experimental protocols approved by the University of California Irvine Animal Care and Use Committee (IACUC). All methods were carried out in accordance with relevant guidelines and recommendations of the IACUC. All methods of euthanasia were carried out in accordance with the American Veterinary Medical Association (AVMA) guidelines. All studies were performed and reported in accordance with the ARRIVE guidelines. Efforts were made to minimize animal numbers and suffering. Both male and female mice from 129S6/SvEvTac strain (Taconic Biosciences) were utilized for preparation of brain slices.

Preparation of acute hippocampal slices.

Slices were prepared from the brains of ~ 4 week old mice (both sexes) as previously described (Medvedeva et al., 2009). Mice were deeply anesthetized with isoflurane and decapitated. The brains were quickly removed and placed in an ice-cold solution containing (in mM): 220 sucrose, 3 KCl, 1.25 NaH_2PO_4 , 6 MgSO_4 , 26 NaHCO_3 , 0.2 CaCl_2 , 10 glucose and 0.42 ketamine (pH 7.35, 310 mOsm, equilibrated with 95% O_2 / 5% CO_2). Horizontal brain slices (300 μm) were cut using a Leica VT1200 vibratome (Leica, Germany) which has close to zero vertical vibration, thereby minimizing damage to the neurons caused by cutting. Slices were placed in artificial cerebro-spinal fluid (ACSF) containing (in mM): 126 NaCl, 3 KCl, 1.25 NaH_2PO_4 , 1 MgSO_4 , 26 NaHCO_3 , 2 CaCl_2 , 10 Glucose (pH 7.35, 310 mOsm, equilibrated with 95% O_2 / 5% CO_2). Slices were incubated for 1 hour at $34 \pm 0.5^\circ\text{C}$, and then kept at room temperature (RT, 20–23°C) in oxygenated ACSF.

Fluorescent measurements.

All recordings were obtained from the pyramidal neuron rich CA1 cell layer of the hippocampus in slices placed on the stage of an Olympus BX51WI microscope (Olympus, Japan) using a 40X objective. Experiments were performed at $32 \pm 0.5^\circ\text{C}$ with a flow speed 2 ml/min. Recordings were carried out from the cell layer 30–50 μm below the slice surface. To investigate the dynamic changes in ROS production, slices were bath loaded with the ROS-sensitive indicator Hydroethidine (HEt, 10 μM , at RT) [24, 32]. HEt was excited at 540(25) nm and emitted fluorescence was collected at 605(55) nm. To assess changes in $\Delta\Psi_m$, slices were bath loaded with Rhodamine 123 (Rhod123, 26 μM , 30 min at RT). Rhod123 is positively charged and accumulates in negatively charged mitochondria where its fluorescence is quenched. Upon loss of $\Delta\Psi_m$ the indicator is released into the cytoplasm causing an increase in fluorescence [33]. Rhod123 was excited at 540(25) nm and emitted fluorescence was collected at 605(55) nm. Carbonyl cyanide-4-(trifluoromethoxy)phenylhydrazone (FCCP, 2 μM) was applied at the indicated time points to evoke full loss of $\Delta\Psi_m$ and consequent maximal increase in Rhod123 fluorescence, providing a measure of the level of $\Delta\Psi_m$ before FCCP application. HEt and Rhod123 images were acquired every 15 s using MetaFluor imaging software (Molecular Devices, San Jose, CA). Data are presented as $\Delta F = (F - F_0)/F_0$ where F is the current fluorescence intensity and F_0 is the baseline fluorescence intensity.

OGD/reperfusion model in slices and drug administration.

To induce ischemia-like conditions in brain slices, ACSF was changed to an identical solution but without glucose (it was substituted with equimolar sucrose to maintain osmolarity) and bubbled with 95% N₂ / 5% CO₂. OGD was terminated after 6 min by restoration of oxygenated ACSF containing glucose, as we found that longer episodes of OGD caused substantial neuronal swelling evoked by spreading depolarization events usually occurring between 6 and 8 min after the start of OGD. This short OGD evoked a substantial burst in ROS production while causing minimal cell swelling.

Experimental drugs [the Zn²⁺ chelator TPEN (N,N,N',N'-tetrakis(2-pyridylmethyl)ethane-1,2-diamine, 20 μM), the MCU inhibitor Ru265 (5 μM), the NOX inhibitor apocynin (500 μM), FTY720 (10 μM), and low-dose FCCP (100 nM)] were applied 0–5 min after OGD withdrawal as indicated. FCCP (2 μM) was applied at the end of some experiments to evoke complete loss of $\Delta\Psi_m$.

Reagents.

Hydroethidine (Dihydroethidium) and FCCP (Carbonyl cyanide 4-(trifluoromethoxy)phenylhydrazone) were purchased from Cayman Chemical (Ann Arbor, MI). FTY720 (fingolimod) was obtained from APExBIO (Boston, MA). Rhodamine123 was obtained from Invitrogen (Carlsbad, CA). TPEN was purchased from Tocris (Bristol, UK), and ketamine was obtained from Sigma (St. Louis, MO). Ru265 was a gift from J. Wilson (Cornell University, Ithaca, NY). All other reagents were purchased from ThermoFisher Scientific (Waltham, MA).

Experimental design and statistical analyses.

Statistical differences were assessed using one-Way ANOVA Tukey test in most of our experiments comprising 3 or more groups of data. In some experiments (when specified in Results section) we used a two-sample t-Test for comparison between two groups. To assess the rate of ROS generation after OGD (Fig. 1C) we evaluated the speed of HEt fluorescence changes by linear fitting of specific areas on the trace (baseline, 20–30 min and 40–60 min intervals after OGD withdrawal). Data were analyzed using Origin software (OriginLab, Northampton, MA). Our preliminary experiments did not find differences of investigated parameters between slices of female and male animals. In particular, we observed a 2-phase increase in ROS generation in animals of both sexes, and found no differences in HEt fluorescence levels at 50 min after the start of OGD between male and female groups (n = 6 males and 9 females, p = 0.97, two-sample t-Test). Thus, all statistical analyses included slices from mice of both sexes. All comparisons reflect sets of data substantially interleaved in time and were based on 7–20 slices from ≥ 6 animals for each condition (numbers of slices are indicated for each experiment).

Results

Ischemia/reperfusion evokes a 2-stage acceleration in ROS production.

Our past studies observed that ROS generation is considerably increased during ischemia [24]. The current study focuses on events occurring after reperfusion – the period most amenable to

interventions. As possibilities for dynamic ROS monitoring are very limited in animal models, we used *ex vivo* slices from adult mice. Slices were loaded with the ROS-sensitive indicator Hydroethidine (HEt) and subjected to short (6 min) OGD followed by reperfusion. Fluorescent measurements were obtained from the CA1 region of hippocampus. We found that OGD/reperfusion causes a pronounced 2-stage acceleration in ROS generation: the first one begins 2–3 min after the start of OGD, lasts for ~ 10 min, and is followed by a marked slowdown; the second stage starts ~ 40 min after OGD withdrawal (Fig. 1a,b) (rate of HEt ΔF changes was $0.07 \pm 0.01\%/min$ at baseline, $0.43 \pm 0.09\%/min$ at 20–30 min interval and $0.94 \pm 0.12\%/min$ between 40 and 60 min, $n = 12$, Fig. 1c).

Mitochondrial hyperpolarization after OGD.

As discussed in the introduction, we hypothesize that OGD/reperfusion evoked Ca^{2+} accumulation in mitochondria causes mitochondrial hyperpolarization after reperfusion, and a resulting remarkable increase in ROS production. We started testing our hypothesis by assessing whether mitochondrial hyperpolarization indeed occurs after OGD. To evaluate $\Delta\Psi_m$ we loaded slices with the fluorescent indicator, Rhodamine 123 (Rhod123) as in our previous studies [25, 26]. This positively charged indicator is sequestered in negatively charged mitochondria, where its fluorescence is quenched, and the accumulated amount is proportional to $\Delta\Psi_m$. After partial or full $\Delta\Psi_m$ loss, Rhod123 is released to the cytoplasm. Treatment with the protonophore FCCP (2 μ M) dissipates the proton gradient across the mitochondrial inner membrane and evokes full $\Delta\Psi_m$ dissipation, leading to Rhod123 release into the cytosol and a corresponding increase in fluorescence (ΔF). This ΔF is indicative of the $\Delta\Psi_m$ prior to FCCP exposure. After subjecting brain slices to the short (6 min) OGD we observed the $\Delta\Psi_m$ loss followed by complete recovery 10–30 min after OGD withdrawal (Fig. 2a). 30 min after the OGD termination we applied FCCP (2 μ M) and found that the resulting increase in Rhod123 ΔF slightly but significantly exceeded that obtained from slices not subjected to OGD (control), indicating hyperpolarization of $\Delta\Psi_m$ after ischemia (Fig. 2b, Rhod123 $\Delta F = 85.3 \pm 3.2\%$, $n = 21$ after ischemia vs $75.3 \pm 3.8\%$ in control, $n = 18$, $p = 0.038$, two-sample t-Test, Fig. 2).

Mild mitochondrial depolarization with low dose FCCP or FTY720 considerably decreases ROS generation after ischemia.

Next, we tested whether a slight $\Delta\Psi_m$ dissipation after reperfusion can mitigate the ROS overproduction. We observed that a low dose of the protonophore FCCP (100 nM) evokes a slight increase in Rhod123 fluorescence ($8.6 \pm 0.8\%$, $n = 8$, data not shown) in the CA1 hippocampal zone indicative of a mild loss of $\Delta\Psi_m$. Subsequently, we found that applying FCCP (100 nM, 5 min after OGD withdrawal for 50 min) considerably decreased the reperfusion-evoked ROS overproduction (HEt $\Delta F = 24.4 \pm 3.2\%$, $n = 13$ slices, vs $39.7 \pm 2.8\%$, $n = 14$ in control (OGD alone), $p < 0.01$, assessed 50 min after OGD onset, Fig. 3a, d).

As FCCP is not suitable as a drug, we searched for another agent capable of mildly depolarizing mitochondria. FTY720 (an FDA approved drug for treatment of multiple sclerosis) was shown to evoke mitochondrial depolarization in cultured cells [34]. In brain slices, we found that 10 μ M of FTY720 causes

a small and reversible mitochondrial depolarization in the hippocampal CA1 zone ($9.40 \pm 0.7\%$, $n = 11$, Fig. 3b). Next, we found that an exposure to FTY720 after OGD termination substantially inhibited the ROS burst after reperfusion (HEt $\Delta F = 25.1 \pm 3.0\%$, $n = 12$ slices, $p < 0.01$ vs control, evaluated 50 min after OGD onset, Fig. 3c, d).

Mitochondrial Zn^{2+} accumulation through the MCU after ischemia contributes to post-ischemic ROS overproduction.

Since our previous studies found substantial and long-lasting Zn^{2+} accumulation in CA1 mitochondria after reperfusion, and also found that Zn^{2+} is a potent contributor to ROS generation by neuronal mitochondria in culture, we questioned whether the Zn^{2+} contributes to the reperfusion-evoked ROS overproduction. Indeed, we found that Zn^{2+} chelation with TPEN applied after OGD termination decreased the late surge in ROS after reperfusion (HEt $\Delta F = 25.7 \pm 2.6\%$, $n = 10$ with TPEN vs $39.7 \pm 2.8\%$, $n = 14$ slices in control, OGD alone, $p = 0.02$, evaluated 50 min after OGD onset, Fig. 4a, e).

Our past studies found that by ~ 30 min after OGD Zn^{2+} is cleared from cytoplasm and accumulates in mitochondria, where it stays for prolonged periods of at least 1 hour [26, 35]. Thus, we sought to assess whether post-ischemic ROS generation depends specifically upon Zn^{2+} entrance to mitochondria. To prevent Zn^{2+} accumulation to mitochondria we blocked the MCU after OGD withdrawal using the recently developed MCU inhibitor Ru265 [36]. Surprisingly, while MCU inhibition changed the dynamics of ROS generation, it also caused an increase in ROS production during first ~ 20 min after OGD, thus having little net effect on the total amount of ROS 50 min after the start of OGD (HEt $\Delta F = 37.7 \pm 3.2\%$, $n = 7$ with Ru265, vs $39.7 \pm 2.8\%$, $n = 14$ in control, $p = 1$, Fig. 4b, e). We hypothesized that since MCU inhibition prevents both Zn^{2+} and Ca^{2+} entrance into mitochondria, it likely causes a greater Ca^{2+} accumulation in the cytoplasm, which can lead to overactivation of NOX – another possible source of ROS after ischemia [5, 37, 38]. Indeed, co-treatment with Ru265 and the NOX inhibitor apocynin largely eliminated the post-ischemic ROS burst (HEt $\Delta F = 25 \pm 2.1$, $n = 7$, vs $39.7 \pm 2.8\%$, $n = 14$ in control, $p < 0.01$, evaluated 50 min after the start of OGD, Fig. 4c, e). Treatment with apocynin alone had a small, non-significant effect on ROS production during reperfusion (HEt $\Delta F = 32.3 \pm 3.7\%$, $n = 8$, $p = 0.13$ compared to control, Fig. 4d, e).

Discussion

While prolonged global ischemia results in immediate brain death, with shorter ischemic episodes neurons often initially recover. However, many sensitive neurons, particularly CA1 hippocampal pyramidal neurons, die within hours to days later. Thus, many deleterious events leading to neuronal death occur after reperfusion, a time when blood flow to the brain is restored and interventions are possible. The role of ROS in reperfusion-associated neuronal injury has long been established by many studies that documented oxidative damage to multiple types of intracellular molecules [15, 17, 39]. Nonetheless, the specific mechanisms and, thus, targets for interventions are largely not understood,

and most of our knowledge about the dynamics of ROS production during and after ischemia originates from experiments utilizing dissociated cultures [5].

Our study used short transient OGD and reperfusion in acute hippocampal slices loaded with the ROS sensitive indicator, HET, to monitor changes in ROS generation. Slices comprise native brain tissue and connectivity and recapitulate many of the events occurring during *in vivo* ischemia while permitting precise environmental control and monitoring of responses. We observed a two-phase acceleration of ROS generation: the first one starts during OGD and continues into early reperfusion, and the second phase is a delayed burst of ROS occurring ~ 40 minutes after OGD termination. We found no prior observations of this “late” burst and, more importantly, barely any information related to possible mechanisms involved in post-ischemic ROS overproduction. As possibilities for intervention are very limited during ischemia, when the first acceleration of ROS production occurs, we investigated the factors contributing to the second, delayed, ROS burst.

As we hypothesized that OGD/reperfusion evoked Ca^{2+} accumulation in mitochondria causes overactivation of the ETC, leading to mitochondrial hyperpolarization and excessive ROS generation, we investigated whether mitochondrial hyperpolarization indeed occurs after reperfusion and contributes to the ROS burst. We found distinct hyperpolarization of $\Delta\Psi_m \sim 30$ min after OGD withdrawal. We further found that treating slices after OGD termination with either low-dose FCCP or FTY720, both of which we found to cause a mild (~ 10%) loss of $\Delta\Psi_m$, largely suppressed the delayed ROS burst – supporting the idea that mitochondrial hyperpolarization after reperfusion is an important contributor to the delayed ROS production.

We also found that Zn^{2+} chelation with TPEN inhibits the late ROS burst, supporting the critical role of Zn^{2+} in post-ischemic ROS production. As our previous studies discovered that after ischemia Zn^{2+} quickly accumulates in CA1 mitochondria [26], we suggest that Zn^{2+} -mediated ROS acceleration after OGD also depend upon Zn^{2+} accumulation to mitochondria. Thus, we assessed whether inhibiting Zn^{2+} entrance to mitochondrial affects ROS generation. Surprisingly, while blocking the MCU attenuated the delayed ROS burst, it appeared to result in accelerated ROS generation at earlier time points after reperfusion (Fig. 4b). We questioned whether this earlier increase in ROS might be because MCU blockade prevents mitochondrial Ca^{2+} buffering resulting in an increased cytosolic Ca^{2+} load which could trigger ROS generation by NOX activation [40]. Indeed, combined application of the MCU inhibitor RU265 with the NOX antagonist, apocynin, strongly attenuated the ROS generation. Apocynin by itself had little effect on the observed delayed ROS burst, suggesting that NOX makes a relatively small contribution to the total ROS production in the absence of MCU blockade.

Mitochondrial Ca^{2+} accumulation is a trigger of reperfusion-associated mitochondrial hyperpolarization and ROS overproduction.

“Excitotoxicity” has long been implicated as a major contributor to ischemic injury. Critical early studies demonstrated that Ca^{2+} entrance through NMDA-activated channels contributes to neuronal injury in

many pathological conditions including ischemia [41–43]. However, clinical trials targeting NMDA receptors failed to result in any substantial protection after ischemia [44, 45]. This can be explained by the fact that most of the Ca^{2+} accumulation occurs during the acute ischemic event when there is little opportunity for intervention. A more beneficial approach would be to target downstream events following ischemic Ca^{2+} accumulation.

Multiple studies found that during ischemia Ca^{2+} quickly accumulates in mitochondria [12–14], and mitochondria were proposed to be important targets for deleterious effects of Ca^{2+} [10, 11, 46]. It has been shown that elevated Ca^{2+} is a potent activator of the mitochondrial respiratory chain causing increased respiration and ROS production [9, 16, 47–49]. This mechanism likely serves as an adaptation to increase ATP production during physiological conditions of high energy demand [46]. However, during pathological ischemic conditions, mitochondrial Ca^{2+} overload probably causes the respiratory chain overactivation but without oxidative phosphorylation and ATP production due to lack of oxygen. Consequently, after reperfusion (upon restoration of oxygen and glucose) overactivation of the ETC likely leads to enhanced and prolonged hyperpolarization of $\Delta\Psi_m$. Sanderson et al. [9] in their comprehensive review proposed that this mitochondrial hyperpolarization contributes to ROS overproduction after ischemia. The idea of the deleterious role of reperfusion-related mitochondrial hyperpolarization was further supported by experiments manipulating the mitochondrial uncoupling protein 2 (UCP2). Deletion of UCP2 increased ROS production and exacerbated brain injury after middle cerebral artery occlusion in mice [50], while UCP2 overexpression protected the brain after cerebral ischemia [51]. Furthermore, several studies found that mitochondrial hyperpolarization causes an exponential increase in ROS production [18, 19, 52].

Mitochondrial Zn^{2+} accumulation after reperfusion contributes to ROS overproduction.

Our previous studies found that long-lasting Zn^{2+} accumulation occurs after ischemia in the mitochondria of highly vulnerable CA1 neurons, but not in CA3 neurons that are more resistant to ischemic injury. Moreover, we also found that this Zn^{2+} accumulation contributes to delayed mitochondrial damage [25, 26]. The mechanism of Zn^{2+} -associated mitochondrial injury was not clear, but studies using cultured neurons and isolated mitochondria found that mitochondrial Zn^{2+} accumulation is an important contributor to ROS generation [23, 27–29]. One of the possible mechanisms is that Zn^{2+} has been shown to cause irreversible inhibition of mitochondrial enzymes of antioxidant defense [30]. A feed-forward process is also likely involved since ROS, in turn, causes more Zn^{2+} to be released from Zn^{2+} -binding proteins such as metallothionein-III resulting in increased mitochondrial Zn^{2+} loading [22, 53]. Furthermore, Zn^{2+} is able to stay in the matrix for hours, likely exacerbating mitochondrial damage [35]. Conversely, we did not find substantial delayed Ca^{2+} accumulation in mitochondria at 30 min and 1 hour after ischemia, likely reflecting mitochondrial ability to clear Ca^{2+} relatively quickly via the $\text{Na}^+/\text{Ca}^{2+}$ exchanger, which is the main mediator of Ca^{2+} release from mitochondria in neurons [26, 54–56]. In conclusion, our observations of long-lasting Zn^{2+}

accumulation in mitochondria after reperfusion and decrease of post-ischemic ROS production by either Zn^{2+} chelation or prevention of Zn^{2+} entrance to mitochondria support a key contribution of mitochondrial Zn^{2+} accumulation after ischemia to oxidative damage of CA1 neurons.

NOX and ischemic ROS generation.

NOX was recently found to be the main source of ROS production after NMDA exposure to cultured neurons [40]. Consistent with this result, while we did not find NOX activation to be a major contributor to reperfusion-evoked ROS generation, our data suggest that NOX is involved, particularly if cytosolic Ca^{2+} is elevated due to block of mitochondrial Ca^{2+} uptake via MCU blockade; thus, targeting NOX in combination with other treatments (like MCU blockade) might be beneficial.

Therapeutic implications.

Therapies for ischemic brain injury are extremely limited for several reasons including: 1) limited knowledge of critical events leading to neuronal injury and death, and 2) inability to deliver drugs to sites of ischemic injury until blood flow is restored. Consequently, the primary focus to date has been to restore blood flow as quickly as possible. However, processes set into motion by even relatively brief (several minute) episodes of ischemia can lead to delayed neuronal injury and death. Oxidative damage due to ROS production has long been felt to be a major contributor to the post-ischemic injury.

Our studies revealed a major burst of mitochondrial ROS production appearing after a delay (~ 40 min) following an episode of acute ischemia. This delay before maximal ROS production may permit delivery of drugs when blood flow is restored after the acute ischemic episode. Present findings suggest 2 mechanisms that appear to contribute importantly to the delayed mitochondrial ROS generation after transient ischemia: hyperpolarization of the mitochondria, to which Ca^{2+} accumulation in mitochondria through the MCU likely contributes, and Zn^{2+} accumulation in mitochondria through the MCU possibly damaging the mitochondria antioxidant system (Fig. 5). Targeting these mechanisms with drugs delivered after reperfusion may provide a valuable new approach for interrupting the pathogenic cascade, thereby resulting in better treatment outcomes.

Study limitations.

A limitation of the study is the absence of ratiometric ROS indicators that can be reliably used in slices. We found that hydroethidine is the most suitable for detecting changes in ROS production in brain slices both at baseline and during ischemia/reperfusion. However as it is non-ratiometric, its fluorescence is affected by short-lasting but substantial cell swelling evoked by spreading depolarization that usually occurs between 6 and 8 min after the start of OGD, and also by slowly developing cell swelling starting at some point after 1 h of reperfusion. This limits both the duration of OGD and time of recording after OGD termination. Additionally, it is possible that slight swelling which can occur in some slices even after 6 min OGD might mask some of the ROS production increase, resulting in underestimations of actual ROS generation changes.

Declarations

Acknowledgements: Supported by NIH grant NS121227 (JHW). We wish to thank Justin Wilson (Cornell University, Ithaca, NY; presently at The University of California, Santa Barbara, Santa Barbara, CA) for the gift of Ru265. The authors declare no competing financial interests.

Data availability

The datasets used and/or analyzed during the current study are available from the corresponding author on reasonable request.

Author Contribution

YM and JW planned the project and wrote the main manuscript text. YM carried out most experiments. ES assisted with data analysis. All authors reviewed the manuscript.

References

1. Petito, C. K., Feldmann, E., Pulsinelli, W. A. & Plum, F. Delayed hippocampal damage in humans following cardiorespiratory arrest. *Neurology* **37**, 1281–1286 (1987).
2. Sugawara, T., Fujimura, M., Morita-Fujimura, Y., Kawase, M. & Chan, P. H. Mitochondrial release of cytochrome c corresponds to the selective vulnerability of hippocampal CA1 neurons in rats after transient global cerebral ischemia. *J. Neurosci.* **19**, RC39 (1999).
3. Chouchani, E. T. et al. Ischaemic accumulation of succinate controls reperfusion injury through mitochondrial ROS. *Nature* **515**, 431–435 (2014).
4. Sugawara, T. & Chan, P. H. Reactive oxygen radicals and pathogenesis of neuronal death after cerebral ischemia. *Antioxid. Redox Signal.* **5**, 597–607 (2003).
5. Abramov, A. Y., Scorziello, A. & Duchen, M. R. Three distinct mechanisms generate oxygen free radicals in neurons and contribute to cell death during anoxia and reoxygenation. *J. Neurosci.* **27**, 1129–1138 (2007).
6. Wingler, K. et al. NOX1, 2, 4, 5: counting out oxidative stress. *Br. J. Pharmacol.* **164**, 866–883 (2011).
7. Yamaguchi, M. et al. The Effects of Xanthine Oxidoreductase Inhibitors on Oxidative Stress Markers following Global Brain Ischemia Reperfusion Injury in C57BL/6 Mice. *PLoS One.* **10**, e0133980 (2015).
8. Piantadosi, C. A. & Zhang, J. Mitochondrial generation of reactive oxygen species after brain ischemia in the rat. *Stroke* **27**, 327–331; discussion 332 (1996).
9. Sanderson, T. H., Reynolds, C. A., Kumar, R., Przyklenk, K. & Huttemann, M. Molecular mechanisms of ischemia-reperfusion injury in brain: pivotal role of the mitochondrial membrane potential in reactive oxygen species generation. *Mol. Neurobiol.* **47**, 9–23 (2013).

10. Dugan, L. L. et al. Mitochondrial production of reactive oxygen species in cortical neurons following exposure to N-methyl-D-aspartate. *J. Neurosci.* **15**, 6377–6388 (1995).
11. Reynolds, I. J. & Hastings, T. G. Glutamate induces the production of reactive oxygen species in cultured forebrain neurons following NMDA receptor activation. *J. Neurosci.* **15**, 3318–3327 (1995).
12. Medvedeva, Y. V., Lin, B., Shuttleworth, C. W. & Weiss, J. H. Intracellular Zn²⁺ accumulation contributes to synaptic failure, mitochondrial depolarization, and cell death in an acute slice oxygen-glucose deprivation model of ischemia. *J. Neurosci.* **29**, 1105–1114 (2009).
13. Puka-Sundvall, M. et al. Subcellular distribution of calcium and ultrastructural changes after cerebral hypoxia-ischemia in immature rats. *Brain Res. Dev. Brain Res.* **125**, 31–41 (2000).
14. Racay, P. et al. Mitochondrial calcium transport and mitochondrial dysfunction after global brain ischemia in rat hippocampus. *Neurochem Res.* **34**, 1469–1478 (2009).
15. Ambrosio, G. et al. Oxygen radicals generated at reflow induce peroxidation of membrane lipids in reperfused hearts. *J. Clin. Invest.* **87**, 2056–2066 (1991).
16. Territo, P. R., Mootha, V. K., French, S. A. & Balaban, R. S. Ca²⁺ activation of heart mitochondrial oxidative phosphorylation: role of the F₀/F₁-ATPase. *Am. J. Physiol. Cell. Physiol.* **278**, C423–435 (2000).
17. Kohr, M. J. et al. Simultaneous measurement of protein oxidation and S-nitrosylation during preconditioning and ischemia/reperfusion injury with resin-assisted capture. *Circ. Res.* **108**, 418–426 (2011).
18. Korshunov, S. S., Skulachev, V. P. & Starkov, A. A. High protonic potential actuates a mechanism of production of reactive oxygen species in mitochondria. *FEBS Lett.* **416**, 15–18 (1997).
19. Liu, S. S. Cooperation of a reactive oxygen cycle with the Q cycle and the proton cycle in the respiratory chain—superoxide generating and cycling mechanisms in mitochondria. *J. Bioenerg Biomembr.* **31**, 367–376 (1999).
20. Koh, J. Y. et al. The role of zinc in selective neuronal death after transient global cerebral ischemia. *Science* **272**, 1013–1016 (1996).
21. Tonder, N., Johansen, F. F., Frederickson, C. J., Zimmer, J. & Diemer, N. H. Possible role of zinc in the selective degeneration of dentate hilar neurons after cerebral ischemia in the adult rat. *Neurosci. Lett.* **109**, 247–252 (1990).
22. Ji, S. G., Medvedeva, Y. V., Wang, H. L., Yin, H. Z. & Weiss, J. H. Mitochondrial Zn²⁺ Accumulation: A Potential Trigger of Hippocampal Ischemic Injury. *Neuroscientist*, 1073858418772548 (2018).
23. Ji, S. G., Medvedeva, Y. V. & Weiss, J. H. Zn²⁺ entry through the mitochondrial calcium uniporter is a critical contributor to mitochondrial dysfunction and neurodegeneration. *Exp. Neurol.* **325**, 113161 (2020).
24. Medvedeva, Y. V. & Weiss, J. H. Intramitochondrial Zn²⁺ accumulation via the Ca²⁺ uniporter contributes to acute ischemic neurodegeneration. *Neurobiol. Dis.* **68**, 137–144 (2014).

25. Medvedeva, Y. V. et al. Blocking mitochondrial Zn(2+) accumulation after ischemia reduces mitochondrial dysfunction and neuronal injury. *J. Neurosci.* **42**, 5281–5292 (2022).
26. Medvedeva, Y. V., Ji, S. G., Yin, H. Z. & Weiss, J. H. Differential Vulnerability of CA1 versus CA3 Pyramidal Neurons After Ischemia: Possible Relationship to Sources of Zn²⁺ Accumulation and Its Entry into and Prolonged Effects on Mitochondria. *J. Neurosci.* **37**, 726–737 (2017).
27. Clausen, A., McClanahan, T., Ji, S. G. & Weiss, J. H. Mechanisms of Rapid Reactive Oxygen Species Generation in response to Cytosolic Ca²⁺ or Zn²⁺ Loads in Cortical Neurons. *Plos One*. **8**, e83347 (2013).
28. Sensi, S. L., Yin, H. Z., Carriedo, S. G., Rao, S. S. & Weiss, J. H. Preferential Zn²⁺ influx through Ca²⁺-permeable AMPA/kainate channels triggers prolonged mitochondrial superoxide production. *Proc. Natl. Acad. Sci. U S A* **96**, 2414–2419 (1999).
29. Sensi, S. L., Yin, H. Z. & Weiss, J. H. AMPA/kainate receptor-triggered Zn²⁺ entry into cortical neurons induces mitochondrial Zn²⁺ uptake and persistent mitochondrial dysfunction. *Eur. J. Neurosci.* **12**, 3813–3818 (2000).
30. Gazaryan, I. G., Krasinskaya, I. P., Kristal, B. S. & Brown, A. M. Zinc irreversibly damages major enzymes of energy production and antioxidant defense prior to mitochondrial permeability transition. *J. Biol. Chem.* **282**, 24373–24380 (2007).
31. Gazaryan, I. G. et al. Zinc is a potent inhibitor of thiol oxidoreductase activity and stimulates reactive oxygen species production by lipoamide dehydrogenase. *J. Biol. Chem.* **277**, 10064–10072 (2002).
32. Bindokas, V. P., Jordan, J., Lee, C. C. & Miller, R. J. Superoxide production in rat hippocampal neurons: selective imaging with hydroethidine. *J. Neurosci.* **16**, 1324–1336 (1996).
33. Duchen, M. R., Surin, A. & Jacobson, J. Imaging mitochondrial function in intact cells. *Methods Enzymol.* **361**, 353–389 (2003).
34. Nagahara, Y., Ikekita, M. & Shinomiya, T. Immunosuppressant FTY720 induces apoptosis by direct induction of permeability transition and release of cytochrome c from mitochondria. *J. Immunol.* **165**, 3250–3259 (2000).
35. Sensi, S. L., Ton-That, D. & Weiss, J. H. Mitochondrial sequestration and Ca(2+)-dependent release of cytosolic Zn(2+) loads in cortical neurons. *Neurobiol. Dis.* **10**, 100–108 (2002).
36. Woods, J. J. et al. A Selective and Cell-Permeable Mitochondrial Calcium Uniporter (MCU) Inhibitor Preserves Mitochondrial Bioenergetics after Hypoxia/Reoxygenation Injury. *ACS Cent. Sci.* **5**, 153–166 (2019).
37. Ma, M. W. et al. NADPH oxidase in brain injury and neurodegenerative disorders. *Mol. Neurodegener.* **12**, 7 (2017).
38. Matsushima, S., Tsutsui, H. & Sadoshima, J. Physiological and pathological functions of NADPH oxidases during myocardial ischemia-reperfusion. *Trends Cardiovasc. Med.* **24**, 202–205 (2014).
39. Kamal, F. Z. et al. The Role of Potential Oxidative Biomarkers in the Prognosis of Acute Ischemic Stroke and the Exploration of Antioxidants as Possible Preventive and Treatment Options. *Int. J. Mol. Sci.* **24**, (2023).

40. Brennan, A. M. et al. NADPH oxidase is the primary source of superoxide induced by NMDA receptor activation. *Nat. Neurosci.* **12**, 857–863 (2009).
41. Choi, D. W. Excitotoxic cell death. *J. Neurobiol.* **23**, 1261–1276 (1992).
42. Meldrum, B. S., Evans, M. C. & Swan, J. H. Simon R. P. Protection against hypoxic/ischaemic brain damage with excitatory amino acid antagonists. *Med. Biol.* **65**, 153–157 (1987).
43. Rothman, S. M. & Olney, J. W. Glutamate and the pathophysiology of hypoxic–ischemic brain damage. *Ann. Neurol.* **19**, 105–111 (1986).
44. Hoyte, L., Barber, P. A., Buchan, A. M. & Hill, M. D. The rise and fall of NMDA antagonists for ischemic stroke. *Curr. Mol. Med.* **4**, 131–136 (2004).
45. Ikonomidou, C. & Turski, L. Why did NMDA receptor antagonists fail clinical trials for stroke and traumatic brain injury? *Lancet Neurol.* **1**, 383–386 (2002).
46. Nicholls, D. G. & Budd, S. L. Mitochondria and neuronal survival. *Physiol. Rev.* **80**, 315–360 (2000).
47. Balaban, R. S. Cardiac energy metabolism homeostasis: role of cytosolic calcium. *J. Mol. Cell. Cardiol.* **34**, 1259–1271 (2002).
48. Hopper, R. K. et al. Mitochondrial matrix phosphoproteome: effect of extra mitochondrial calcium. *Biochemistry* **45**, 2524–2536 (2006).
49. Huttemann, M. et al. Regulation of oxidative phosphorylation, the mitochondrial membrane potential, and their role in human disease. *J. Bioenerg Biomembr.* **40**, 445–456 (2008).
50. He, M. et al. Deletion of mitochondrial uncoupling protein 2 exacerbates mitophagy and cell apoptosis after cerebral ischemia and reperfusion injury in mice. *Int. J. Med. Sci.* **17**, 2869–2878 (2020).
51. Haines, B. & Li, P. A. Overexpression of mitochondrial uncoupling protein 2 inhibits inflammatory cytokines and activates cell survival factors after cerebral ischemia. *PLoS One.* **7**, e31739 (2012).
52. Starkov, A. A. & Fiskum, G. Regulation of brain mitochondrial H₂O₂ production by membrane potential and NAD(P)H redox state. *J. Neurochem.* **86**, 1101–1107 (2003).
53. Stork, C. J. & Li, Y. V. Elevated Cytoplasmic Free Zinc and Increased Reactive Oxygen Species Generation in the Context of Brain Injury. *Acta Neurochir. Suppl.* **121**, 347–353 (2016).
54. Baron, K. T. & Thayer, S. A. CGP37157 modulates mitochondrial Ca²⁺ + homeostasis in cultured rat dorsal root ganglion neurons. *Eur. J. Pharmacol.* **340**, 295–300 (1997).
55. David, G. Mitochondrial clearance of cytosolic Ca(2+) in stimulated lizard motor nerve terminals proceeds without progressive elevation of mitochondrial matrix [Ca(2+)]. *J. Neurosci.* **19**, 7495–7506 (1999).
56. Medvedeva, Y. V., Kim, M. S. & Usachev, Y. M. Mechanisms of prolonged presynaptic Ca²⁺ + signaling and glutamate release induced by TRPV1 activation in rat sensory neurons. *J. Neurosci.* **28**, 5295–5311 (2008).

Figures

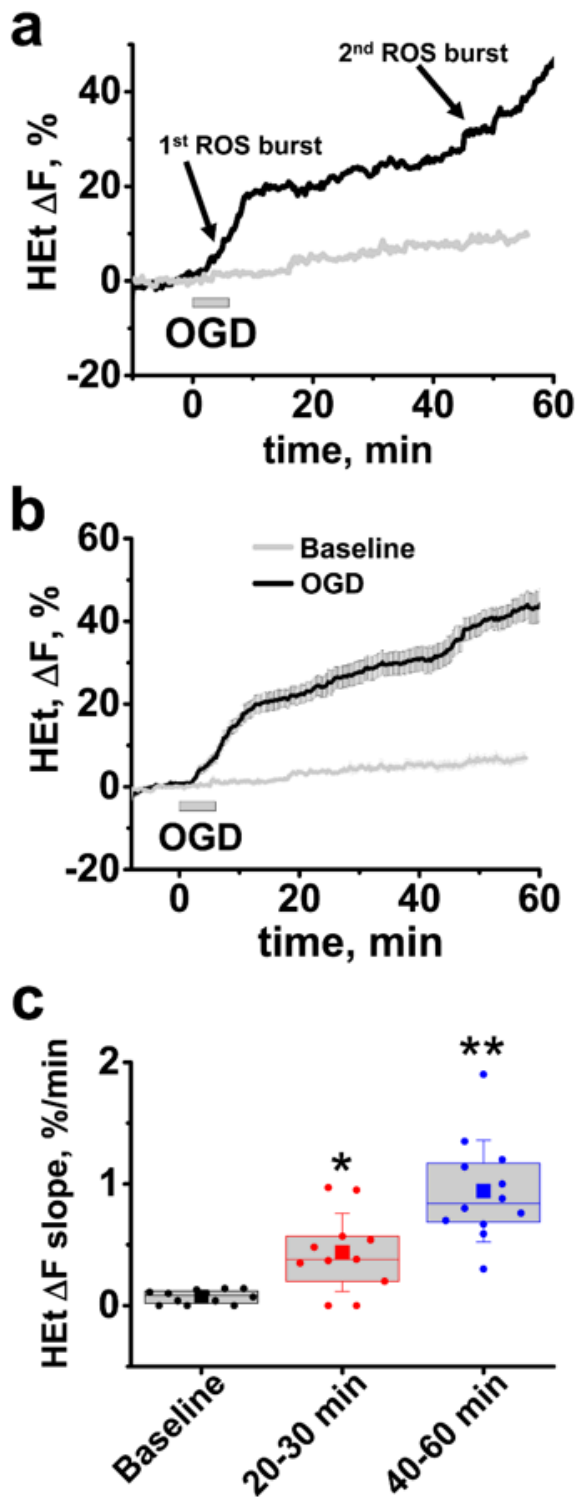


Figure 1

OGD/reperfusion evokes a two-phase acceleration in ROS production. Slices were bath loaded with HET and subjected to OGD/reperfusion. Traces demonstrate dynamic changes in HET fluorescence in the CA1 zone of hippocampus during OGD/reperfusion (black traces) and in slices not subjected to treatment (gray traces) in a representative slice (**a**) and as an average (\pm SE) of 14 slices (**b**). **c** Box chart represents the average rate of HET ΔF changes (with borders at the 25th and 75th percentile, presented as % per

min) during baseline, and during 2 time intervals – from 20-30 min, and from 40-60 min after OGD withdrawal. Circle symbols show data points for individual slices, squares show mean value, central line demonstrate median, and error bars show SD of mean. * $p < 0.019$ vs baseline, ** $p < 0.01$ compared to both baseline and 20-30 min intervals.

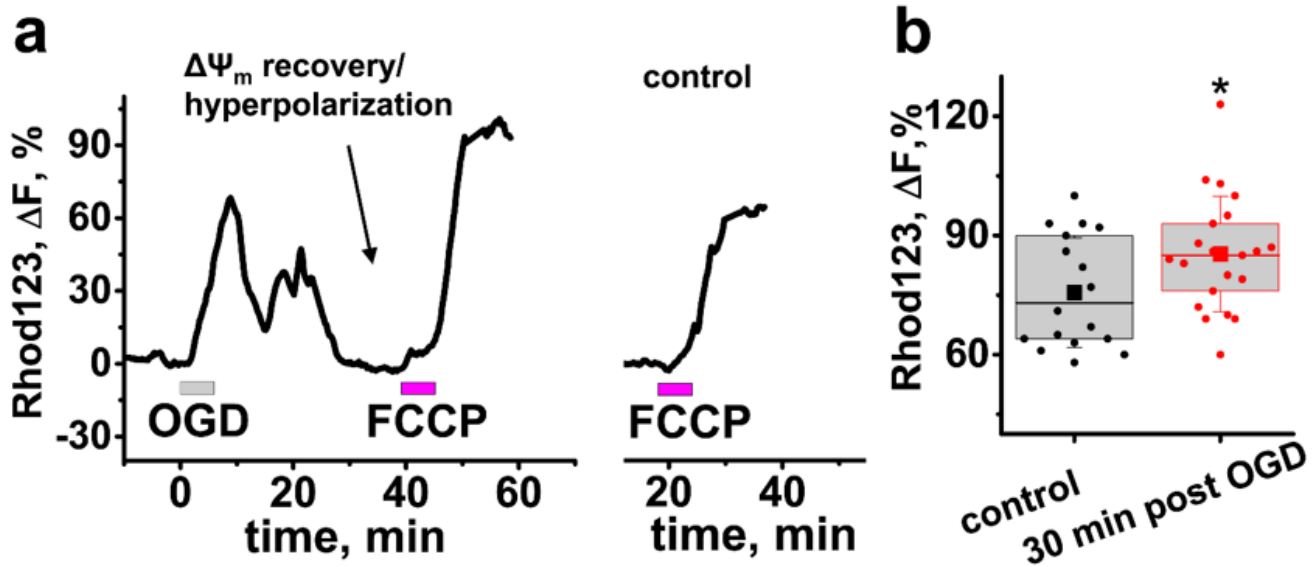


Figure 2

Mitochondria are moderately hyperpolarized 30 min after OGD withdrawal. Slices were loaded with Rhod123. **a** Representative traces show changes of Rhod123 fluorescence in the CA1 pyramidal cell zone of a slice exposed to OGD followed 30 min later by FCCP (2 mM, **Left**), or in a control slice treated with FCCP only (**Right**). **b** Box chart represents Rhod123 fluorescence changes in response to FCCP treatment (these changes are indicative of the $\Delta\Psi_m$ prior to FCCP exposure) in slices ~30 min after an OGD episode or in control untreated slices. The square symbol points to average, borders show 25th and 75th percentiles, circle symbols show data points for individual slices, and error bars indicate standard deviation. , * - $p = 0.038$ vs control

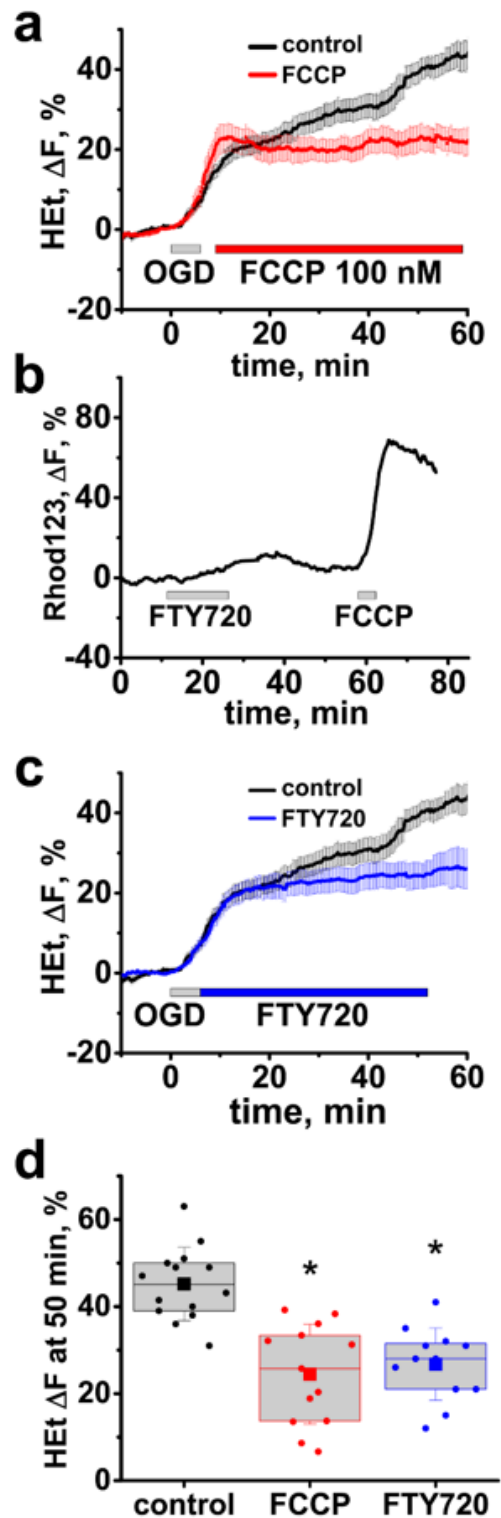


Figure 3

Mild mitochondrial depolarization inhibits the reperfusion evoked ROS burst in CA1. **a** Low dose FCCP (100 nM) decreases ROS generation after OGD. Slices were bath loaded with H_{Et} and subjected to short OGD followed by application of FCCP 5 min later. Traces show average (\pm SE) changes in H_{Et} DF in control slices subjected to OGD alone (black) and in slices treated with FCCP (red). **b** FTY720 causes a slight and reversible loss of $\Delta\Psi_m$. Slices were bath loaded with Rhod123. Representative trace (from

n=11) show changes in Rhod123 fluorescence after application of FTY720 (10 μ M) for 15 min followed by FCCP (2 μ M) 30 min later, as indicated. **c** FTY720 inhibits the reperfusion-evoked ROS generation. Traces show average changes in HEt fluorescence in control slices (black) and in slices treated with FTY720 (blue, 10 μ M) after OGD termination, as indicated. **d** Box chart shows average (square symbol, borders are at 25th and 75th percentiles) HEt DF 50 min after the start of the OGD episode in control slices and in slices treated with FCCP or FTY720. Circle symbols show data points for individual slices, and error bars indicate standard deviation. * - $p<0.01$ vs control

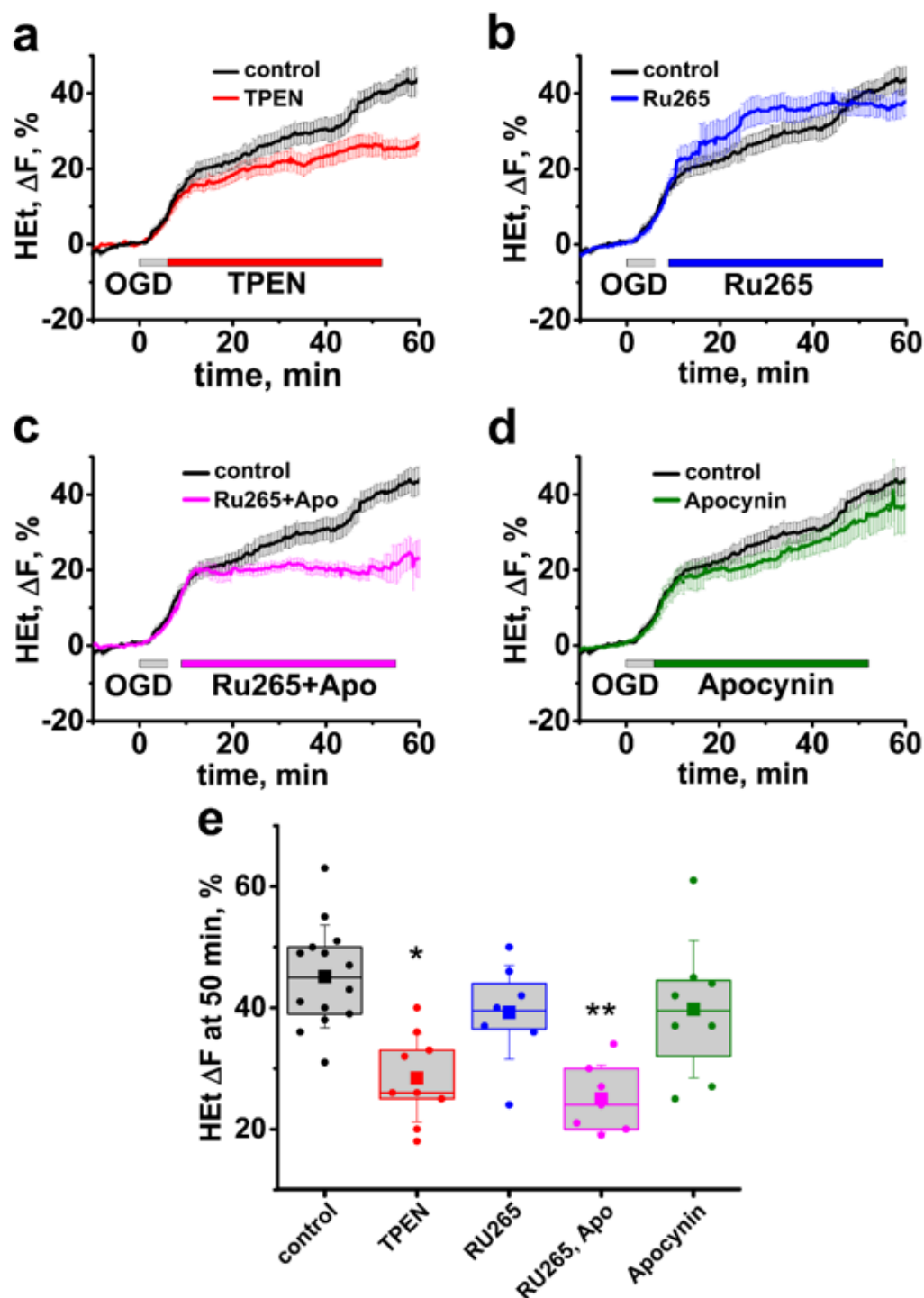


Figure 4

Mitochondrial Ca^{2+} and Zn^{2+} accumulation through the MCU contribute to the post-ischemic ROS overproduction. **a-d** Average traces show changes in HEt fluorescence in control slices subjected to OGD alone (black trace) and in experiments where treatments were administered *after OGD withdrawal*, as indicated. **a** Zn^{2+} chelation with TPEN after OGD (red trace) attenuates the sharp increase in ROS generation. **b** MCU inhibition with RU265 changes dynamics but does not decrease ROS production (blue trace). **c** MCU blockade combined with inhibition of NOX by apocynin considerably diminishes the reperfusion-evoked ROS burst (magenta trace). **d** NOX inhibition alone (olive) does not notably affect ROS. **e** Box chart shows average HEt DF 50 min after the start of OGD. * - $p=0.02$, ** - $p<0.01$ vs control

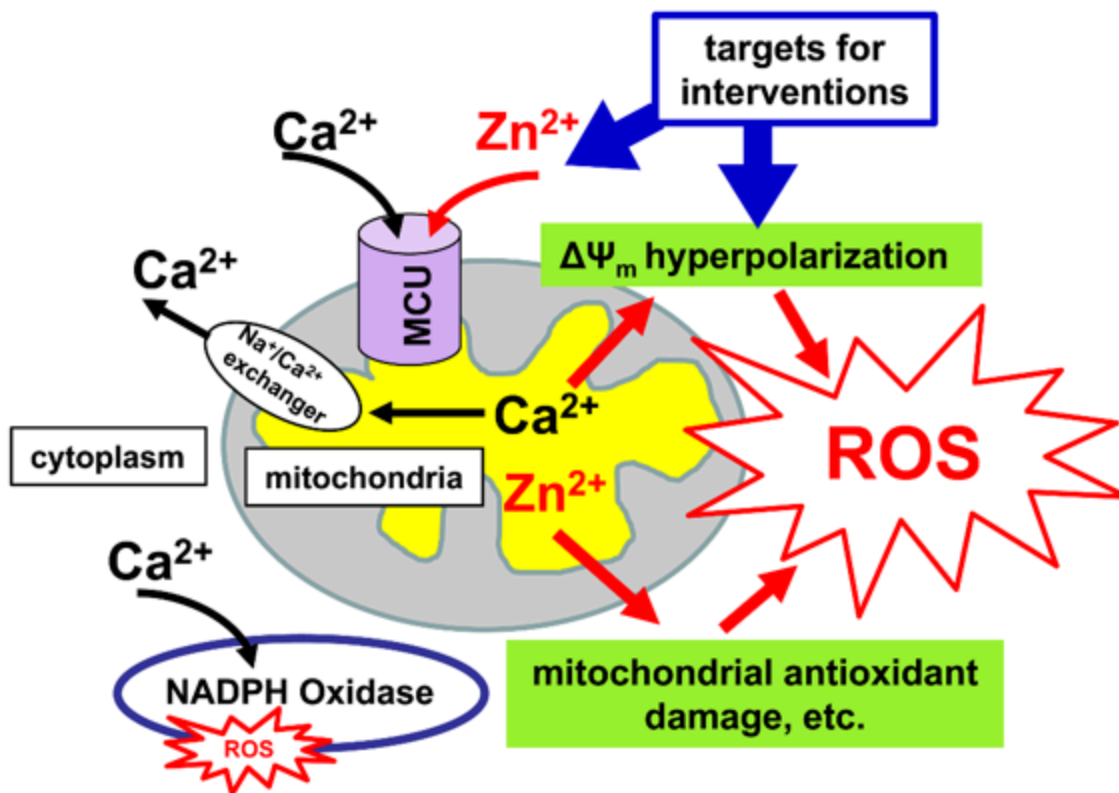


Figure 5

Events likely occurring after ischemia and contributing to ROS production. Mitochondria repolarize/hyperpolarize and commence reuptake of Zn^{2+} and Ca^{2+} (These ions initially enter mitochondria during ischemia and are released into cytosol upon loss of $\Delta\Psi_m$.) Ca^{2+} is then released from mitochondria through the $\text{Na}^+/\text{Ca}^{2+}$ exchanger, but Ca^{2+} triggered overactivation of the ETC and consequent mitochondrial hyperpolarization causes accelerated ROS production. In the cytoplasm Ca^{2+} can activate NOX, which causes additional ROS generation. Zn^{2+} stays in mitochondria for a prolonged period of time, causing mitochondrial dysfunction and contributing to the delayed ROS burst. The mitochondrial hyperpolarization and the Zn^{2+} accumulation in mitochondria (possibly in combination with NOX inhibition) can be targeted after restoration of blood flow to prevent excessive ROS generation

